

# THE ROLE OF SIRT2 IN $\alpha$ -TUBULIN, TAU AND $\alpha$ -SYNUCLEIN POST-TRANSLATIONAL MODIFICATIONS IN PARKINSON'S DISEASE

A. Palma<sup>1</sup>, A.R. Esteves<sup>2</sup>, D. Santos<sup>2</sup>, C. Januário<sup>3</sup>, S.M. Cardoso<sup>1,2\*</sup>

<sup>1</sup>Faculty of Medicine, University of Coimbra, Coimbra, Portugal;

<sup>2</sup>CNC–Center for Neuroscience and Cell Biology, University of Coimbra, Portugal;

<sup>3</sup>Neurology Department, Coimbra University Hospital Centre (CHUC), Coimbra, Portugal.

\* To whom correspondence should be addressed to Dr. Sandra Morais Cardoso, CNC – Center for Neuroscience and Cell Biology, University of Coimbra, Largo Marquês de Pombal 3004-517 Coimbra, Portugal; E-mail address: cardoso.sandra.m@gmail.com.

## ABSTRACT

Sporadic Parkinson's disease (sPD) is characterized by mitochondrial dysfunction and the accumulation of protein aggregates in a specific group of neurons. It has already been demonstrated by our group that microtubule (MT) - dependent dynamics disruption due to mitochondrial dysfunction have a major role in sPD etiopathogenesis.

Given that the MT network is disrupted in sPD cells and that microtubule associated proteins (MAPs) allow MT stabilization we aim to clarify the role of Sirtuin-2 (SIRT2), a NAD<sup>+</sup> dependent protein that deacetylates  $\alpha$ -tubulin in PD cellular neurodegeneration.

We used human neuroblastoma SHSY-5Y cell lines that overexpressed  $\alpha$ -synuclein (ASYN) and transmitochondrial cybrids that recapitulate pathogenic alterations observed in sPD patient brains. We confirmed that Tau protein and ASYN are MT-associated proteins.

Moreover, our results suggested that  $\alpha$ -tubulin acetylation induced by SIRT2 inhibition is functionally associated with the improvement of MT dynamic determined by decrease in phospho-Tau levels, or by increase in Tau/Tubulin and ASYN/tubulin binding. Our data provide a strong evidence for a functional role of tubulin and MAPs acetylation on autophagic vesicular traffic and cargos clearance. Additionally, we showed that an inherited mitochondrial dysfunction (sPD cybrids) or an accumulation of ASYN oligomers (overexpressed ASYN cells) imbalance mitochondrial fusion and fission events which further compromised autophagy.

Moreover, this study indicates that MT can be a promising therapeutic target in the field of neurodegenerative disorders, like sPD, in which intracellular transport is altered.

## **RESUMO**

Os casos esporádicos da doença de Parkinson (sPD) são caracterizados por disfunção mitocondrial, assim como, pela acumulação de agregados proteicos num grupo específico de neurónios. Já foi previamente demonstrado pelo nosso grupo que, a alteração dos mecanismos mediados por microtúbulos (MTs) em consequência da disfunção mitocondrial, tem um papel importante na etiopatogenia do sPD.

Dado que a rede de MT está alterada nas células de doentes com sPD e que as proteínas associadas a microtúbulos (MAPs) permitem a estabilização dessa rede de MT, nós pretendemos clarificar o papel desempenhado pela Sirtuina-2, uma proteína dependente de NAD<sup>+</sup> que induz a desacetilação da  $\alpha$ -tubulina logo alterando a estabilidade dos MTs.

Nós utilizámos células de neuroblastoma humano (SHSY-5Y) que sobreexpressam  $\alpha$ -sinucleína (ASYN) e cíbridos transmitocondriais que recapitulam as alterações patogénicas observadas nos cérebros de sPD. Confirmámos que a proteína Tau e a ASYN são proteínas

associadas aos microtúbulos. Os nossos resultados sugerem, inclusivamente, que os níveis de acetilação da  $\alpha$ -tubulina estão associados à melhoria da dinâmica dos MT, evidenciada quer pelo decréscimo dos níveis de proteína Tau fosforilada, quer pelo aumento da interacção entre Tau/ $\alpha$ -tubulina e ASYN/ $\alpha$ -tubulina em células tratadas com um inibidor de SIRT2. Os nossos resultados sugerem fortemente que a acetilação da  $\alpha$ -tubulina e das proteínas MAPs tem uma elevada importância funcional no transporte de vesículas autofágicas, assim como na eliminação de mitocôndrias disfuncionais e agregados proteicos. Demonstrámos também que, tanto a disfunção mitocondrial (cíbridos de sPD), como a acumulação de oligómeros de ASYN (células que sobreexpressam ASYN) promovem uma alteração dos mecanismos de fissão e fusão mitocondriais comprometendo a autofagia.

Assim sendo, este estudo aponta para os MT como sendo um alvo terapêutico promissor no campo das doenças neurodegenerativas, como o sPD, em que o transporte intracelular está alterado.

## **KEYWORDS**

Parkinson's disease; mitochondria metabolism; sirtuin-2; microtubules acetylation; macroautophagy; Tau and  $\alpha$ -synuclein.

## INTRODUCTION

Parkinson's disease (PD) is the second most common neurodegenerative disorder and the most common neurodegenerative movement disorder. PD is chronically progressive, age-related and clinically characterized by progressive resting tremor, rigidity, bradykinesia, gait disturbance, postural instability and dementia. The major neuropathological hallmark of PD is the loss of dopaminergic neurons in the substantia nigra pars compacta (SNpc) leading to a dopamine deficit in the striatum. A second neuropathological feature is the presence of intracytoplasmic inclusions (Lewy bodies, LBs) which comprise a dense core of different proteins, the main one is  $\alpha$ -synuclein (ASYN), but there are other proteins like parkin, ubiquitin, synphilin-1, tubulin. (1)

Understanding the molecular basis of PD has proven to be a major challenge in the field of neurodegenerative diseases. Although several hypotheses have been proposed to explain the molecular mechanisms underlying the pathogenesis of PD, a growing body of evidence has highlighted the role of mitochondria and of microtubule (MT) - dependent dynamics disruption as a major contributor to PD etiopathogenesis. Mitochondrial association with idiopathic PD was first established when a mitochondrial NADH dehydrogenase (complex I) activity deficit was identified in the SNpc of postmortem PD patients brains (2) and in PD patients platelets (3). In addition, mtDNA involvement in complex I defects observed in PD platelets was further recognized after transference of platelets mitochondria into mtDNA deficient cell lines and validated in the resultant cell lines known as "cybrids" (4). Data obtained using this *ex vivo* cellular model has shown that several pathogenic features observed in PD patients brains are actually recapitulated by PD cybrids (5,6). Mitochondria are no long featured as isolated rigid organelles, and indeed, they constantly divide and fuse with each other in a process regulated by Drp 1 and Fis 1 for mitochondrial fission and Opa 1,

Mfn 1 and Mfn2 for mitochondrial fusion (7,8). In fact, besides mitochondrial dysfunction, an imbalance between mitochondrial fission and fusion process has been recently associated with the neurodegenerative process in PD (7-12).

Mitochondrial function and the axonal transport are intimately connected, in fact mitochondria supply the energy that is required to allow molecular motors to move along MT and transport mitochondria, autophagic and synaptic vesicles, as well as some proteins like ASYN (13). Although the mechanism whereby ASYN accumulates in LBs is not fully understood, evidence suggests that defective axonal transport of ASYN may itself contribute to the process. The association between ASYN aggregation and MT stability was supported by the discovery that sirtuin-2 (SIRT2) inhibition changes the characteristics of the intracytoplasmic inclusions and protected against ASYN-induced cytotoxicity (14). In fact, it was previously described by our group that in sPD mitochondrial dysfunction, causes the increase of cytosolic NAD<sup>+</sup>, which induces the activation of SIRT2 (Esteves et al., submitted). SIRT2 is a cytoplasmic class III histone deacetylase that interacts with and deacetylates MTs *in vitro* and *in vivo* (15,16). MTs are regulated by post-translational modifications of tubulin subunits, such as acetylation of the Lys40 residue of  $\alpha$ -tubulin. Indeed, acetylation has been associated with stable MTs, although this relationship has not been clearly proven. In fact there are some studies which support the theory that acetylation enhances MT stability (17,18) whereas others have suggested that acetylation occurs only on stable MTs, but the acetylation itself does not stabilize MTs (19). Based on those facts we hypothesized that the decreased of acetylated tubulin causes an impairment of MT and the disruption of the intracellular trafficking. Under this context, autophagy will not occur in proper conditions causing the accumulation of impaired mitochondria, autophagic vesicles and protein aggregates. All this culminates in the disturbance of synapses. MT network

disruption was also described for the rare cases of familial forms of PD with a mutation in the coding gene for ASYN (20).

Overall we propose that the neurodegenerative process in PD is due to the interplay between mitochondrial dysfunction and MT-dependent traffic disruption, which contribute to an impaired autophagic clearance. Furthermore, we elucidated the molecular framework that correlate the impaired mitochondrial dynamics with MT disassembly, highlighting Tau and ASYN acetylation involvement as well as their interaction with MTs. Herein we expect to provide possible biological therapeutic approaches for PD by improving MT network and consequently enhancing autophagic neuroprotective functions, which are usually altered in PD cell models and brain.

## **MATERIAL AND METHODS**

**Chemicals:** Ammonium chloride ( $\text{NH}_4\text{Cl}$ ) was from Merck KGaA (Darmstadt, Germany). Leupeptin was from Sigma Chemical Co (St. Louis, MO, USA). Ak1 was from ChemBridge Corporation (San Diego, USA). Carbonyl cyanide-p-trifluoromethoxyphenylhydrazone (FCCP) and  $\text{MPP}^+$  were purchased from Sigma (St. Louis, MO, USA).

**Human Subjects:** sPD patients and healthy individuals were recruited after approval by the CHUC Institutional Review Board. The mean age of the PD subjects ( $n=2$ ) who participated in this study was  $64\pm 12.8$  years, and for the control subjects ( $n=2$ ) was  $74.3\pm 5.5$  years. Individuals in the PD group were followed regularly in a tertiary referral movement disorders clinic at CHUC and met criteria commonly used to diagnose PD in clinical and research settings (21). None of the PD subjects were believed to have alternative diagnoses, degeneration of related systems, drug-induced parkinsonism, or any other serious medical illness. Enrolment was also contingent on the absence of a diagnosis for another neurodegenerative disease. The control subjects have not been diagnosed with a neurodegenerative or pre-neurodegenerative disease condition.

**Preparation of platelet mitochondria:** Following provision of informed consent, 60 ml of blood was collected through venipuncture in tubes containing acid-citrate-dextrose as an anticoagulant. Mitochondria were obtained from the human platelets according to previously described methods (22). Platelet mitochondria protein concentrations were measured by the Bradford protein assay (23), in which bovine serum albumin was used as the standard.

**Creation of cybrid cell lines:** To create the cybrid cell lines for this study, we used NT2 (Ntera2/D1) cells, a teratocarcinoma cell line with neuronal characteristics (Stratagene, La Jolla, CA) (24,25). These cells were depleted of endogenous mtDNA (NT2 rho0 cells) via long-term ethidium bromide exposure (26,27). NT2 rho0 cells lack intact mtDNA, do not possess a functional electron transport chain, and are auxotrophic for pyruvate and uridine. Consequently, platelet mitochondria from either PD or control subjects were isolated from the individual blood samples and were used to repopulate NT2 rho0 cells with mtDNA as previously described (26,27). We generate control and disease cell lines at the same point in time and only compared a disease series with a control series that had been made at the same time and with the same immediate stock of NT2 rho0 cells. Briefly, NT2 rho0 cells were co-incubated with polyethylene glycol (Merck Chemicals) with platelets from the human subjects (28). After that the resulting mixture was grown in Rho0 medium in T75 flasks. Seven days after plating, untransformed cells were removed by withdrawal of pyruvate and uridine from the culture medium and substitution of dialyzed, heat inactivated fetal calf serum for non-dialyzed, heat inactivated fetal calf serum (29,30). Maintaining cells in selection medium removes rho0 cells that have not repopulated with platelet mtDNA. Moreover, “mock fusions” in which NT2 rho0 cells were not incubated with platelets were plated and maintained in selection medium in parallel with the true fusions. During the selection period all cells from “mock fusions” died. After selection was complete, the resultant cybrid cells were switched to cybrid growth medium. Flasks were maintained in this medium in a humidified incubator at 37°C and 5% CO<sub>2</sub>. We used 2 sPD and 2 control cybrid cell lines for the experiments where we measured the amount of P-Tau in the presence of AK1. In the immunoprecipitation of ASYN assay we used 1 sPD and 1 control cybrid cell lines.

**Cell line culture and experimental treatments:** Optimem and Dulbecco's modified Eagle's medium (DMEM), as well as Non-dialyzed and dialyzed Fetal Bovine Serum (FBS) were obtained from Gibco-Invitrogen (Life Technologies Ltd, UK). NT2 rho0 cell growth medium Optimem was supplemented with 10% non-dialyzed FBS, 200 µg/ml sodium pyruvate from Sigma (St. Louis, MO, USA), 100 µg/ml uridine from Sigma (St. Louis, MO, USA) and 1% penicillin-streptomycin solution. Cybrid growth medium consisted of Optimem supplemented with 10% non-dialyzed FBS and 1% penicillin-streptomycin solution. Prior to experiments, cell lines were maintained in the cybrid growth medium. For Western Blotting and immunoprecipitation analysis, cybrid cell lines were seeded in petri-dishes at a density of  $0,5 \times 10^6$  cells/well. After 24h the medium was refreshed and experimental treatments were performed. AK1 was prepared in DMSO and was added for 24h to the culture medium with a final concentration of 5 µM. MPP<sup>+</sup> was prepared in water and was added for 24h to the culture medium with a final concentration of 1mM. For immunocytochemistry analysis, cybrid cell lines were grown on coverslips in 12-well plates at a density of  $0,1 \times 10^6$  cells/well. Human neuroblastoma SHSY-5Y cell lines (ATCC-CRL-2266) were grown in 75 cm<sup>2</sup> tissue flasks in RPMI 1640 with 10% FBS , 2mM L-glutamine and antibiotics like 250 µg/ml Geneticin, 50 µg/ml Hygromycin B and also the selection antibiotic 2 µg/mL Doxycycline hyclate (DOX). The presence of DOX represses ASYN and the absence of this antibiotic induces ASYN expression. Cells were maintained at 37°C in a humidified incubator under an atmosphere of 95% air and 5% CO<sub>2</sub>. For Western blotting and immunoprecipitation analysis cells were plated in 6-well plates at a density  $0,5 \times 10^6$  cells/well. For immunocytochemistry analysis, cells were grown on coverslips in 12-well plates at density of  $0.05 \times 10^6$  cells/coverslip. After 24h the medium was refreshed and experimental treatments were performed. AK1 was prepared in DMSO and was added for 24h to the culture medium with a final concentration of 5 µM. Where indicated 20 mM NH<sub>4</sub>Cl and/or 100 µM leupeptin (Sigma, St. Louis, MO,

USA), were added for 4h to the culture medium. The combination of  $\text{NH}_4\text{Cl}$  with leupeptin blocks all types of autophagy, as it reduces the activity of all lysosomal proteases by increasing the lysosomal lumen pH without affecting the activity of other intracellular proteolysis systems (31). FCCP was prepared in DMSO and was added for 2h to the culture medium with a final concentration of  $10\mu\text{m}$ .

**Western blot analysis:** For the analysis of p-Tau Thr 181, p-Tau Ser 396, acetylated  $\alpha$ -tubulin and LC3B, individual cybrid cell lines and SHSY-5Y cell lines were scrapped in buffer containing 25mM HEPES , 1mM EDTA, 1mM EGTA, 2mM MgCl, protease inhibitors (commercial protease inhibitors from Sigma), phosphatase inhibitors (2mM NaF and 50mM sodium orthovanadat), 0,1 PMSF (Sigma), 0,2 M DTT (Sigma) and 1% Triton X-100. Cell suspensions were frozen three times in liquid nitrogen and centrifuged at  $20,000 \times g$  for 10 min. The resulting supernatants were removed and stored at  $-80^\circ\text{C}$ . Protein concentrations were determined by the Pierce<sup>TM</sup> BCA Protein Assay Kit and equal amounts of protein (30 or 60  $\mu\text{g}$ ) were resuspended in 6x sample buffer (4x Tris.Cl/SDS, pH6.8, 30% glycerol, 10% SDS, 0,6 M DTT, 0.012% bromophenol blue) and separated under reducing conditions. p-Tau Thr 181, p-Tau Ser396 and acetylated  $\alpha$ -tubulin samples were loaded onto 10% SDS-PAGE and LC3B samples were loaded onto 15% SDS-PAGE. The samples from the immunoprecipitation assay were loaded onto 12% SDS-PAGE (for ASYN) and onto 10% SDS-PAGE (for  $\alpha$ -tubulin). After samples being resolved by electrophoresis in SDS polyacrylamide gels an transferred to PVDF membranes, non-specific binding was blocked by gently agitating the membranes in 5% non-fat milk or 5% BSA for phosphorylated proteins and 0,1% Tween in TBS for 1h at room temperature. The blots were subsequently incubated with the respective primary antibodies overnight at  $4^\circ\text{C}$  with gentle agitation: 1:1000 monoclonal anti-Tau from Sigma (St. Louis, MO, USA), 1:10000 monoclonal anti- $\alpha$ -tubulin

from Sigma (St. Louis, MO, USA), 1:250 polyclonal anti-p-Tau (Thr 181) from Santa Cruz Biotechnology (Santa Cruz, CA, USA), 1:750 polyclonal anti-p-Tau (Ser 396) from Santa Cruz Biotechnology (Santa Cruz, CA, USA), 1:20000 monoclonal anti-acetylated Tubulin from Sigma (St. Louis, MO, USA), 1:5000 monoclonal anti- $\beta$ -Actin from Sigma (St. Louis, MO, USA), 1:1000 polyclonal anti-LC3B from Cell Signaling (Danvers, MA, USA), 1:1000 polyclonal anti-acetylated-lysine from Cell Signaling Technology, 1:1000 polyclonal rabbit anti-phospho-Drp 1 (Ser616) from Cell Signaling Technology, 1:750 polyclonal rabbit anti-Fis1 from Imgenex, 1:520 polyclonal rabbit anti-OPA1 from Abcam, 1:200 polyclonal rabbit anti-Drp1 from Santa Cruz Biotechnology (Santa Cruz, CA, USA), 1:200 polyclonal rabbit anti-Mfn1 from Santa Cruz Biotechnology (Santa Cruz, CA, USA), 1:200 polyclonal anti-Tom20 from Santa Cruz Biotechnology (Santa Cruz, CA, USA), 1:500 monoclonal mouse anti-Mfn2 antibody from Abnova, 1:500 monoclonal mouse anti-glyceraldehyde-3-phosphate dehydrogenase from Millipore and 1:5000 anti-Hsp60 from BD Transduction Laboratories . Membrane were washed with TBS containing 0,1% Tween three times (each time for 10 min), and then incubated with the appropriate horseradish peroxidase-conjugated secondary antibody for 2h at room temperature with gentle agitation. After three washes specific bands of interest were detected by developing with an alkaline phosphatase enhanced chemical fluorescence reagent (ECF from GE Healthcare). Fluorescence signals were detected using a Biorad Versa-Doc Imager, and band densities were determined using Quantity One Software.

**Immunoprecipitation assay:** Cells were scraped and lysed on ice in a non-denaturing lysis buffer [20 mM Tris-HCl (pH 7.0), 100 mM NaCl, 2 mM EDTA, 2 mM EGTA, supplemented with 0.1% SDS, 1% Triton X-100, 2 mM DTT, 0.1 mM PMSF and a 1:1000 dilution of a protease inhibitor cocktail]. Cellular suspensions were centrifuged at 20,000 x g, 10min at 4°C and whole lysates were assayed for protein concentration by the Pierce<sup>TM</sup> BCA Protein

Assay Kit. 500 µg of each sample were pre-cleared with Protein A Sepharose beads (GE Healthcare Bio-Sciences, Uppsala, Sweden) for 1 h, 4°C, and then incubated with primary antibody, overnight at 4°C and with rotation. The primary antibodies used were: 1:100 monoclonal anti-ASYN (211) from Santa Cruz Biotechnology (Santa Cruz, CA, USA) and 1:10,000 monoclonal anti  $\alpha$ -tubulin from Sigma (St. Louis, MO, USA). Protein A–Sepharose beads were then added to samples followed by 2 h incubation. The beads were spin down and washed seven times in washing buffer [1% Triton X-100, 500 mM NaCl, 2 mM EDTA, 2 mM EGTA, 20 mM Tris-HCl (pH 7.0)]. The last supernatant was collected and 25 µl of 2x sample buffer was added. The samples were boiled at 95-100°C for 5 min to denature the protein and to separate it from the protein-A beads. The boiled proteins were centrifuged at 20,000 x g for 5 min at room temperature and the supernatants collected. Samples were separated by SDS–PAGE and subjected to Western blotting as aforementioned.

**Immunocytochemistry and Confocal microscopy analysis:** Cells were all plated at density of  $0.1 \times 10^6$  cells/well, and after incubation periods, cells were washed two time with PBS 1x and fixed for 30 min at room temperature using 4 % paraformaldehyde. The fixed cells were washed again with PBS 1× three times and permeabilized with 0.2 % Triton X-100 for 2 min. Subsequently, cells were washed three times with PBS 1× and blocked with 3 % BSA for 30 min. Cells were then washed again three times with PBS 1× and then incubated with primary antibody [(1:100 polyclonal anti-Tom20 from Santa Cruz Biotechnology (Santa Cruz, CA, USA) overnight and then with the appropriate secondary antibody 1:250 Alexa Fluor 594 from Molecular Probes (Eugene, OR, USA)]. For MitoTracker Green, cells were washed two times with PBS and incubated with 500 nm MitoTracker Green for 45 min at 37 °C. Cells were then washed two times with PBS and fixed for 30 min at room temperature in 4 % paraformaldehyde. After that, cybrid cell lines were incubated with Hoescth 15 µg/µl for

5 min at room temperature and protected from light. Cells were then washed two times in PBS, and the coverslips were immobilized on a glass slide with mounting medium DakoCytomation (Dako, Glostrup, Denmark). Images were acquired on a Zeiss LSM510 META confocal microscope ( $\times 63$  1.4NA plan-apochromat oil immersion lens) by using Zeiss LSM510 v3.2 software (Carl Zeiss Inc., Thornwood, NY, USA) and analyzed using Zeiss LSM Image Examiner. As previously described by Dagda and colleagues (32), to quantify two parameters of mitochondrial morphology, an ImageJ macro was used. The cells stained with Tom20 were extracted to grayscale, inverted to show mitochondria-specific fluorescence as black pixels and thresholded to optimally resolve individual mitochondria. This macro traces mitochondrial outlines using “analyze particles.” The area/perimeter ratio was employed as an index of mitochondrial interconnectivity, and inverse roundness was used as a measure of mitochondrial elongation.

**Data analysis:** Data provided are the mean  $\pm$  SE of at least duplicates of one independent measurement. Statistical analyses were conducted using one-way ANOVA. Post hoc Bonferroni testing was also performed. Differences were considered statistically significant at  $p < 0.05$ .

## RESULTS

### **The role of specific inhibition of SIRT2 on MT network impairments in sPD cybrid cells**

We investigated the role of SIRT2 deacetylase on cytoskeleton integrity in our cell models. Since SIRT2 interacts with and deacetylates MTs *in vitro* and *in vivo* (15,16), we determined the acetylation state of  $\alpha$ -tubulin and analyze the effects of AK1, an inhibitor that specifically blocks the activity of SIRT2.

Under basal conditions, sPD cybrids showed decreased acetylation levels at Lys40 of  $\alpha$ -tubulin relative to CT cybrids. Treatment with AK1 significantly restored the acetylation of  $\alpha$ -tubulin in sPD cybrids (Fig.1 A and D). Acetylation has been associated with stable MTs, therefore, we considered that AK1 could contribute to prevent MT network impairments.

In order to establish the effects of the inhibition of SIRT2 on MT stability, we determined the degree of affinity of Tau protein to  $\alpha$ -tubulin, based on the principle that the binding of Tau protein to the  $\alpha$ -tubulin contributes to MT structural integrity. It's already known that there's a correlation between the levels of pTau and the degree of affinity of Tau protein to  $\alpha$ -tubulin, in fact, the higher amount of pTau lowers the binding of Tau protein to  $\alpha$ -tubulin (33). Based on this principle, we measured the levels of Tau phosphorylated at Ser396 and at Thr181 (pTau Ser 396 and pTau Thr181) (Fig.1 A-C). Under basal conditions, sPD cybrids showed increased pTau levels relative to CT cybrids. Treatment with AK1 reduced the levels of pTau Ser 396 and pTau Thr 181. This effect was more obvious for pTau Thr181, which was decreased in both CT and sPD cybrid cells. Based on these results, we can hypothesize that under the treatment with AK1 the Tau protein is binding more to  $\alpha$ -tubulin, which could be a protective factor for PD.

We also wanted to know if ASYN could be a MAP. We observed that in sPD cells both ASYN and  $\alpha$ -tubulin are less acetylated, which could imply a decreased interaction between ASYN and  $\alpha$ -tubulin (Fig.1 E-H). Treatment with AK1 significantly increased the interaction between ASYN and  $\alpha$ -tubulin in both, sPD and CT cybrids (Fig.1 E and F). Assuming that the binding of ASYN to  $\alpha$ -tubulin promotes the MT stabilization, this is another argument that corroborates the fact that the inhibition of SIRT2 prevents disruption of the intracellular trafficking by increasing the acetylation levels of ASYN in both, sPD and CT cybrids.

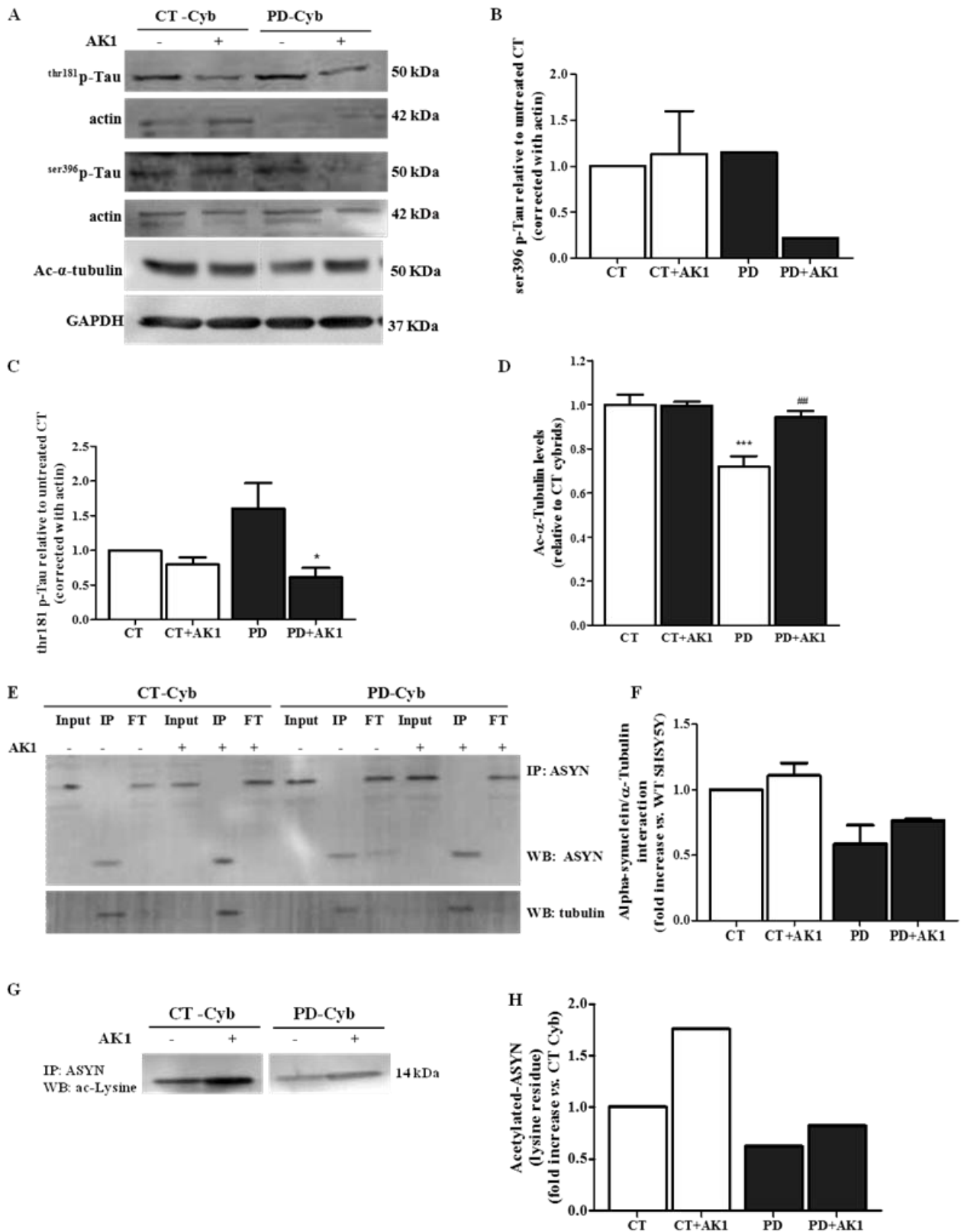


**Figure 1 – The effect of specific inhibition of SIRT2 on tubulin and MAP proteins in sporadic PD cybrids.**

**A)** CT and sPD cybrids were treated with or without AK-1 (5  $\mu$ M, 24 h) and then a western blot analysis was performed using the primary antibodies for p-tau Thr 181, p-tau Ser396 and acetylated  $\alpha$ -tubulin. The blots were probed for actin or GAPDH to confirm equal protein loading; **B)** Densitometry showing that the treatment with

AK1 significantly reduced the levels of pTau Ser 396 in sPD (n=1-2); **C**) Densitometry showing that the treatment with AK1 significantly reduced the levels of p-tau Thr 181 in sPD (n=3); **D**) Densitometry showing that the treatment with AK1 significantly restored the acetylation of  $\alpha$ -tubulin in sPD (n=5); **E**) Immunoprecipitation of ASYN from CT and sPD cybrids that were treated with or without AK-1 (5  $\mu$ M, 24 h). Levels of ASYN (top) and  $\alpha$ -tubulin (bottom) in the input, immunoprecipitate (IP) and flow through (FT) are shown; **F**) Determination of ASYN/ $\alpha$ -tubulin physical interaction (n=2). Treatment with AK1 significantly increased the interaction between ASYN and  $\alpha$ -tubulin in both, sPD and CT cybrids; **G,H**) Western Blot analysis and respective densitometry showing that after the treatment with AK1 there was an increased in the acetylation levels of ASYN in both, sPD and CT cybrids. Data is reported as the fold increase over untreated CT cybrids (n=1). \*p<0.05, \*\*p<0.01, \*\*\*p<0.001, when compared to CT cybrid group and <sup>##</sup>p<0.01, when compared to AK-1 treated CT cybrid.

## **The role of specific inhibition of SIRT2 in MT network impairments in ASYN overexpressing cells**

We also analyzed the effects of the specific inhibition of SIRT2 by AK1 in human neuroblastoma SHSY-5Y cell line expressing ASYN. As a control we performed immunocytochemistry against ASYN and it was evident that SHSY-5Y cell line overexpressing ASYN contained aggregated ASYN (Fig.2 A). Similar to what we did in the previous cell model, we quantified the acetylation state of  $\alpha$ -tubulin after AK1 treatment. We observed that  $\alpha$ -tubulin, under basal conditions, in the ASYN overexpressing cells is less acetylated than in WT cells. Treatment with AK1 significantly restored the acetylation of  $\alpha$ -tubulin on ASYN overexpressing cells (Fig.2 B and D). As aforementioned, acetylation has been associated with stable MTs, therefore, we considered that the specific inhibition of SIRT2 could contribute to prevent MT network impairments. Because the effect of the treatment with AK1 was more obvious on the levels of pTau Thr181 in the previous model, we only quantified pTau Thr181. Under basal conditions, ASYN overexpressing cells showed increased pTau levels relative to WT cells. Treatment with AK1 significantly reduced the levels of pTau Thr 181 (Fig.2 B and C). To complete the study on the affinity of Tau protein to  $\alpha$ -tubulin under the treatment with Ak1 we immunoprecipitated Tau and then performed a Western Blot to detect  $\alpha$ -tubulin levels (Fig.2 E). Under basal conditions, ASYN overexpressing cells showed decreased interaction between Tau protein and  $\alpha$ -tubulin when compared to WT cells. Treatment with AK1 significantly increased the interaction between Tau protein and  $\alpha$ -tubulin in both, ASYN overexpressing cells and WT cells (Fig.2 E and F). Tau protein is a MAP with the function of stabilizing the MT, consequently the increased of the interaction between Tau protein and  $\alpha$ -tubulin promoted by AK1 may be a protective factor for PD.

Finally, we wanted to know if ASYN is binding more or less to  $\alpha$ -tubulin upon increased acetylation with AK1. We immunoprecipitated ASYN and then performed a Western Blot to detect  $\alpha$ -tubulin levels (Fig.2 G). Under basal conditions, ASYN overexpressing cells showed decreased interaction between ASYN and  $\alpha$ -tubulin when compared to WT cells. Treatment with AK1 increased the interaction between ASYN and  $\alpha$ -tubulin in ASYN overexpressing cells (Fig.2 H).

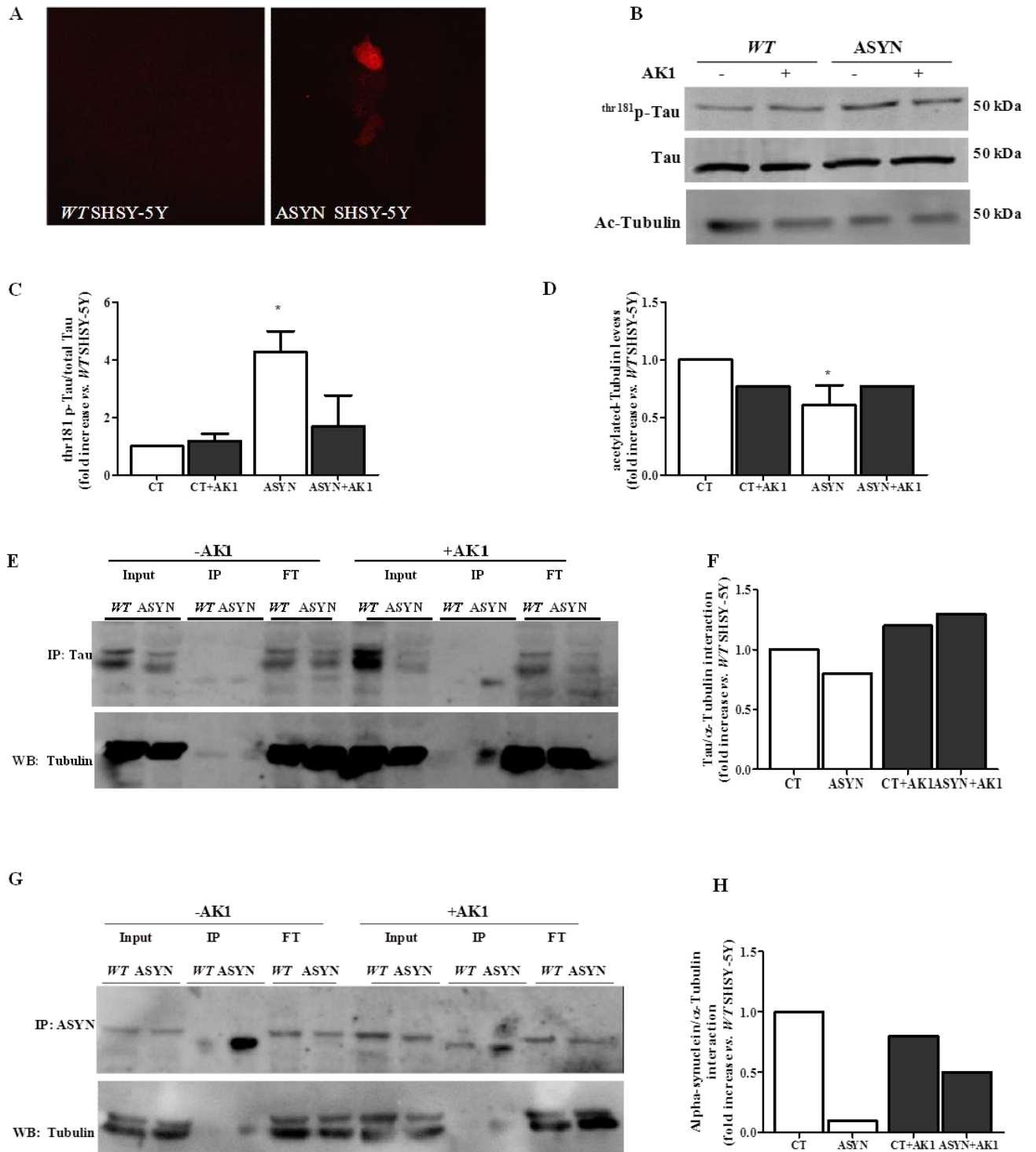


**Figure 2 - The effect of specific inhibition of SIRT2 on tubulin and MAP proteins in ASYN overexpressing cells.**

**A)** Immunocytochemistry against ASYN. The data show that SHSY-5Y wild-type cell line had less ASYN levels compared with SHSY-5Y cell line overexpressing ASYN (n=1); **B)** WT and ASYN overexpressing cells were treated with or without AK-1 (5 μM, 24 h) and then a western blot analysis was performed using the primary antibodies for p-tau Thr 181 and acetylated α-tubulin. The p-tau Thr 181 blot was reprobbed for Tau to confirm equal protein loading; **C)** Densitometry showing that the treatment with AK1 significantly reduced the

levels of p-tau Thr 181 in ASYN overexpressing cells ( $n=3$ ); **D**) Densitometry showing that the treatment with AK1 significantly restored the acetylation of  $\alpha$ -tubulin in ASYN overexpressing cells ( $n=1-2$ ); **E**) Immunoprecipitation of Tau from WT and ASYN overexpressing cells that were treated with or without AK-1 (5  $\mu$ M, 24 h). Levels of Tau (top) and  $\alpha$ -tubulin (bottom) in the input, immunoprecipitate (IP) and flow through (FT) are shown; **F**) Determination of Tau/ $\alpha$ -tubulin physical interaction ( $n=1$ ). Treatment with AK1 significantly increased the interaction between Tau protein and  $\alpha$ -tubulin in both, SHSY-5Y cell lines and WT cells; **G**) Immunoprecipitation of ASYN from WT and ASYN overexpressing cells that were treated with or without AK-1 (5  $\mu$ M, 24 h). Levels of ASYN (top) and  $\alpha$ -tubulin (bottom) in the input, immunoprecipitate (IP) and flow through (FT) are shown; **H**) Determination of ASYN/ $\alpha$ -tubulin physical interaction ( $n=1$ ). Treatment with AK1 significantly increased the interaction between ASYN protein and  $\alpha$ -tubulin. Data is reported as the fold increase over untreated WT cells. \* $p<0.05$ , when compared to WT SHSY-5Y cells.

## **Specific inhibition of SIRT2 improves the autophagic turnover in sPD cybrids and ASYN overexpressing cells**

Autophagic turnover relies on stable MT, in fact mature autophagosomes move along these tracks in order to be degraded (34). It has already been proven by our team that in sPD cybrids there is a disruption of autophagic turnover, which is associated with MT impairment (35). Since, SIRT2 deacetylase regulates MT assembly and knowing that increasing the acetylation at lysine 40 of  $\alpha$ -tubulin enhances the affinity of MAPs, such as Tau and possibly ASYN, we wanted to know if the blockage of SIRT2 activity could improve the autophagic turnover in sPD cybrids and in ASYN overexpressing cells. In order to determine that, we evaluated autophagosome accumulation of LC3-II, a autophagosome marker and its turnover. Since LC3-II is partially degraded by lysosomal hydrolases, following autophagosome-lysosome fusion, increased LC3-II might represent a reduced rate of fusion and LC3-II clearance rather than increased autophagy. To address this question we monitored the autophagic flux, the process from autophagosome formation to degradation, comparing the accumulation of autophagosomes after inhibition of lysosomal function (with  $\text{NH}_4\text{Cl}$  and leupeptin) to the steady-state levels (Fig.3 A and D). With this approach we observed that, under basal conditions, sPD cybrids have an increase in the levels of LC3-II (Fig.3 B) and both PD cybrids and ASYN overexpressing cells have lower autophagic flux (Fig.3 C and F) when compared to CT cells and WT cells respectively. Treatment with AK1, further activated autophagic flux in sPD cybrids and in ASYN overexpressing cells.

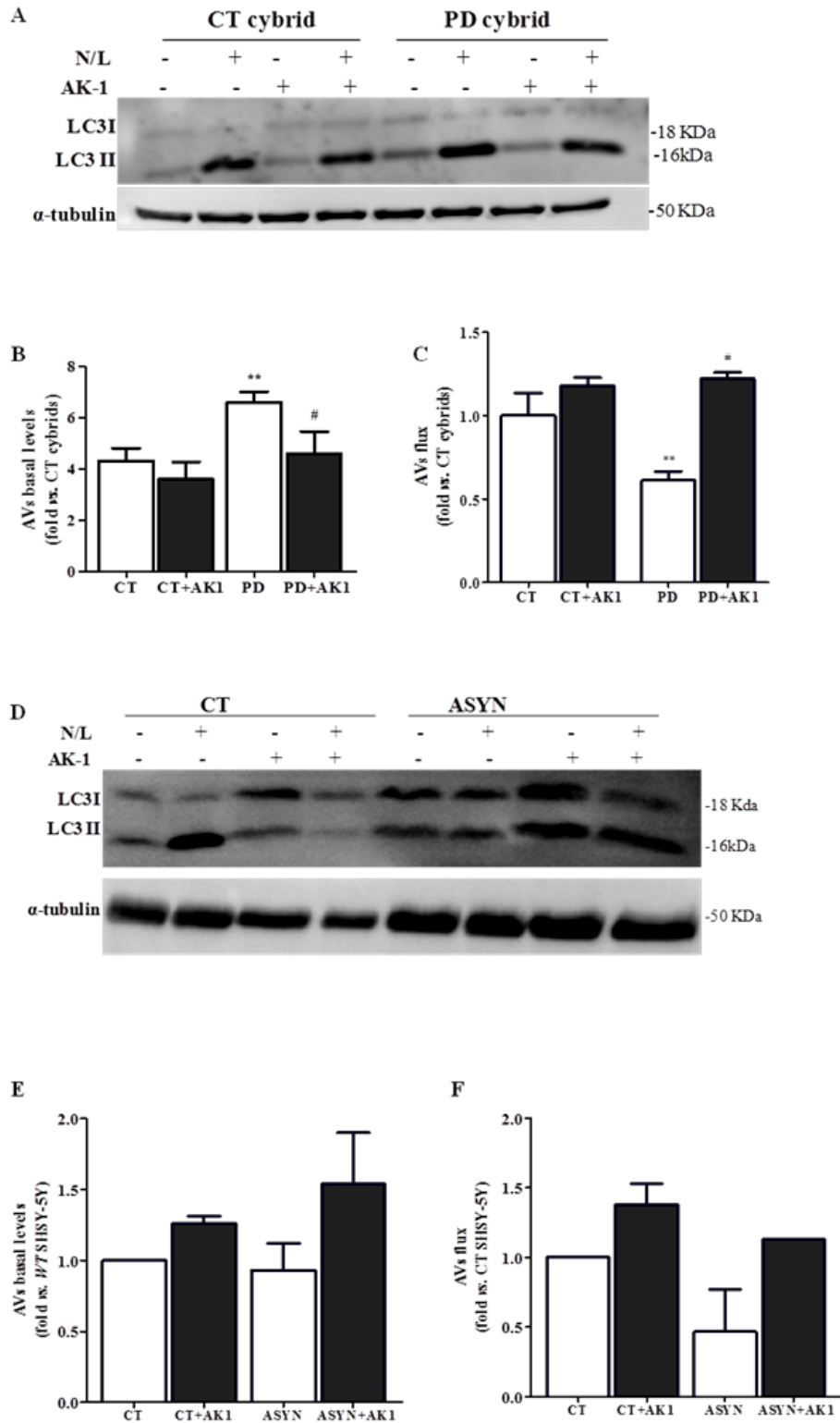


**Figure 3 – Evaluation of the autophagic turnover in sPD cybrids and ASYN overexpressing cells under the specific inhibition of Sirt2.**

**A)** Immunoblot for endogenous LC3-II from CT and PD cybrids treated with or without AK-1 (5  $\mu$ M, 24 h) following culture in the presence or absence of lysosomal inhibitors (N/L - NH<sub>4</sub>Cl and Leupeptin) for the last 4 h. The blots were reprobated for  $\alpha$ -tubulin to confirm equal protein loading; **B)** Densitometric analysis of

endogenous levels of LC3II, data is reported as absolute values (n=7); **C**) Assessment of autophagic flux, calculated as the ratio of LC3II densitometric value of N/L treated samples over the corresponding untreated samples (n=3-10). AK1-treated PD cybrid cells showed an increase in autophagic flux. Data is reported as the fold increase over untreated CT cybrids; **D**) Immunoblot for endogenous LC3-II from WT and ASYN overexpressing cells treated with or without AK-1 (5  $\mu$ M, 24 h) following culture in the presence or absence of lysosomal inhibitors (N/L - NH<sub>4</sub>Cl and Leupeptin) for the last 4 h. The blots were reprobed for  $\alpha$ -tubulin to confirm equal protein loading (n=2); **E**) Densitometric analysis of endogenous levels of LC3B, data is reported as absolute values (n=3); **F**) Assessment of autophagic flux, calculated as the ratio of LC3-II densitometric value of N/L treated samples over the corresponding untreated samples (n=1-2). AK1-treated ASYN overexpressing cells showed an increase in autophagic flux. Data is reported as the fold increase over untreated CT cybrids or WT cells. \*\*p<0.01, when compared to WT SHSY-5Y and #p<0.05, when compared to AK-1 treated WT SHSY-5Y.

## **Mitochondria dynamics in ASYN overexpressing cells and PD cybrids**

Mitochondrial function, transport and degradation rely on mitochondrial fission and fusion events and are dependent of MT assembly (9). It has already been described in previous works that an alteration in mitochondrial network is associated with sPD (9-12). Therefore we wanted to evaluate whether mitochondrial network and dynamics is affected in our cellular models with a compromised MTs.

We used SHSY-5Y overexpressing ASYN cell line and PD cybrids. To evaluate the mitochondrial network, immunocytochemistry was performed against the mitochondrial protein Tom 20, this procedure evidenced a more perinuclear distribution of the mitochondrial network in PD cybrids (Fig.4), in contrast to what was observed in CT cybrids that showed mitochondrial interconnectivity and elongation, with a reticular network. Interestingly, ASYN overexpressing cells contained a more interconnected mitochondrial network as compared to WT cells (Fig. 6). As positive controls, we exposed WT cells to FCCP (Fig. 6) and exposed CT cybrids to MPP<sup>+</sup> - inducing CXI inhibition (Fig. 4). FCCP is an uncoupling agent because it disrupts ATP synthesis by transporting hydrogen ions through a cell membrane before they can be used to provide the energy for oxidative phosphorylation (OXPHOS) whereas MPP<sup>+</sup> is a mitochondrial toxin that induces Parkinsonism in humans, primates and mice by inhibiting complex I of the mitochondrial respiratory chain which causes anatomically specific degeneration of SNpc and locus coeruleus catecholaminergic neurons (36-38). As expected, in both control cell lines, we observed a more dramatically fragmented mitochondria network, resulting in the appearance of round-shaped disconnected mitochondria (Fig.4 and 6).

The observed abnormal mitochondrial network could be due to a disturbance of the proteins involved in the mitochondrial fission/fusion process. To distinguish between these possibilities we evaluated the proteomics of the proteins involved in the mitochondrial fission

and fusion process. Given the slight differences in the protein levels between ASYN overexpressing cells and WT cells, as well as, between PD cybrids and CT cybrids (data not shown), we next asked whether the subcellular localization of the proteins was dissimilar. For this purpose, cells were fractionated in mitochondrial and cytosolic extracts. The results from the fractionation process and the quantification of the proteins involved in mitochondrial dynamic revealed that PD cybrids have a significant reduction in mitochondrial levels of the pro-fusion proteins Opa1, when compared CT cells. Moreover, a statically significant increase in mitochondrial Ser616-pDrp1 was observed. However, no significant differences were seen in the levels of the other proteins in both fractions, inclusive in mitochondrial Mfn1, Mfn2 and Fis1 levels (Fig. 5). Our results strongly suggest that mitochondria are unable to fuse under these conditions, which point toward an increase in mitochondrial fragmentation, hindering elongation and interconnectivity. Accordingly to what was observed in ASYN overexpressing cells regarding an increase in mitochondrial interconnectivity (Fig. 6) we observed an increase in mitochondrial levels of the pro-fusion proteins Opa1 and Mfn1 when compared WT cells. Moreover, a decrease in mitochondrial in Ser616-pDrp1 was observed in ASYN overexpressing cells (Fig. 7).

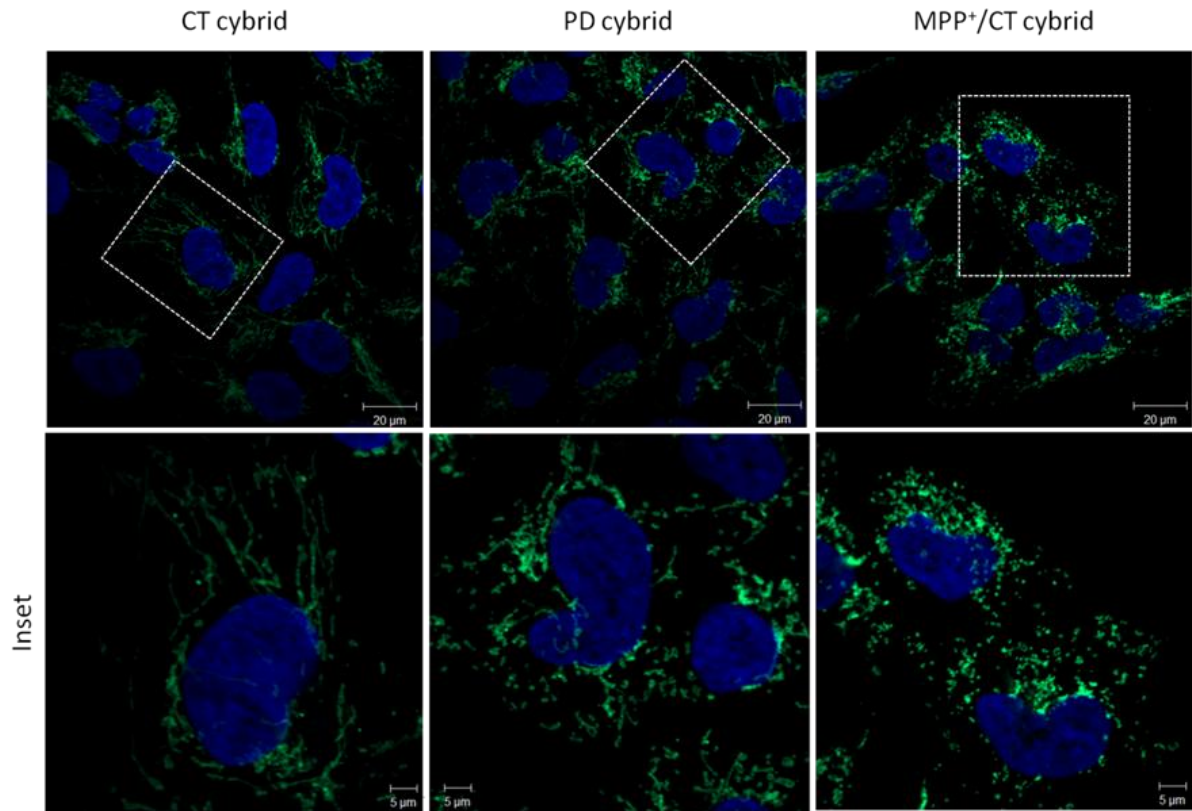


**Figure 4 – Mitochondrial fragmentation and altered distribution in PD cellular models.**

Representative immunofluorescence pictures evidencing mitochondrial network in CT and PD Cybrids, under basal conditions, and in MPP<sup>+</sup>-treated CT cybrids (1mM, 24 hours). Immunocytochemistry was performed against the mitochondrial protein Tom20. PD cybrids and MPP<sup>+</sup>-treated CT cybrids show pronounced mitochondrial fragmentation and perinuclear distribution as opposite to the interconnected well distributed CT cybrids mitochondrial network. Green: Tom20, Blue: Hoechst. (Magnification x63) (Published by Santos et al, 2014).

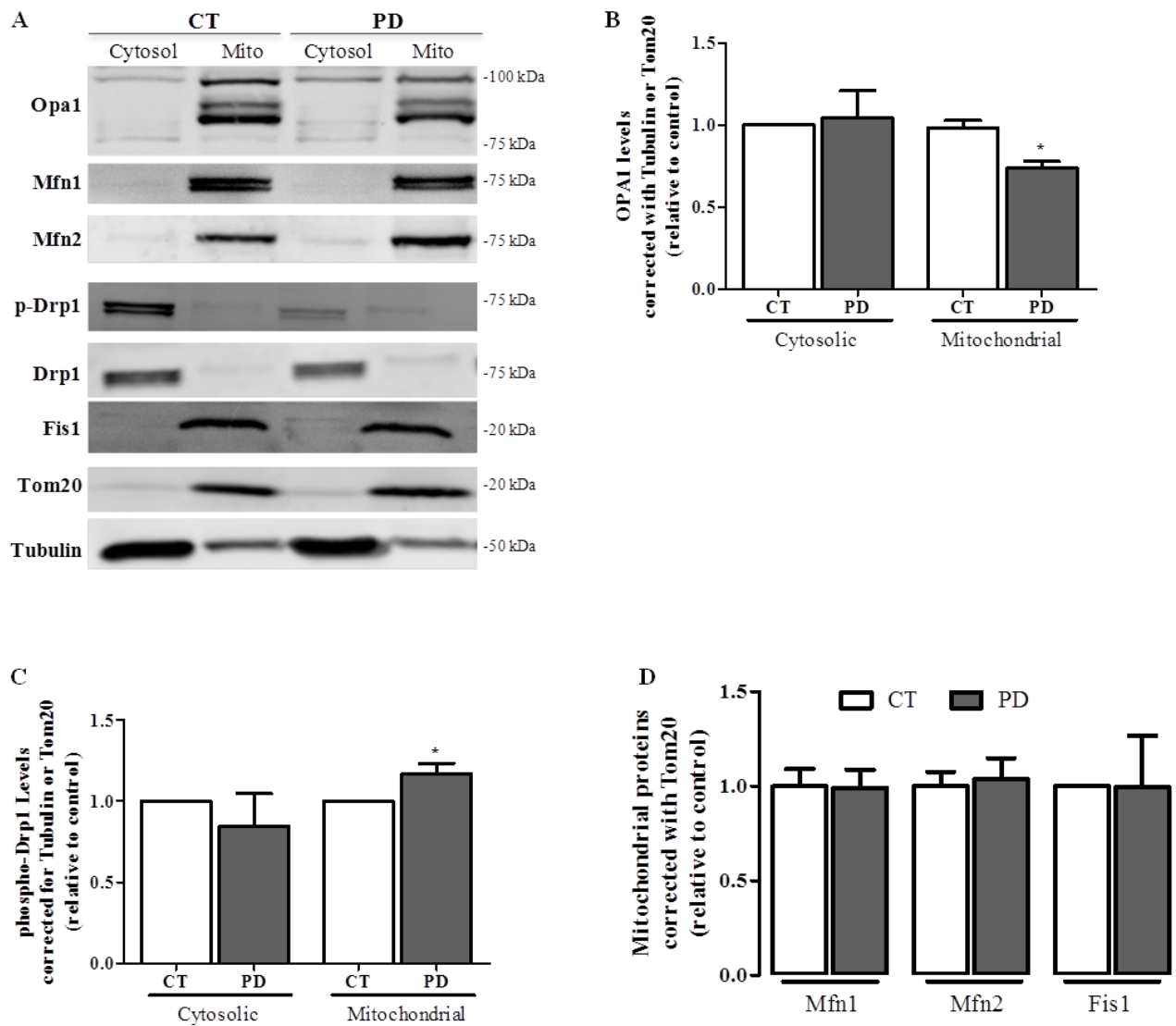


**Figure 5 - Impaired mitochondrial fusion in sporadic PD cybrids.**

CT and PD cybrids cells were harvested and fractionated into mitochondrial and cytosolic fractions. A) Representative immunoblot; B-D) Densitometric analysis of the proteins levels involved in mitochondrial fission and fusion revealed a decrease in the mitochondrial levels of the profusion Opa1 (n=4), an increase in the mitochondrial levels of pro-fission p-Drp1 (n=3) and no alteration in mitochondrial Mfn1, Mfn2 or Fis1 levels (n=4). Equal protein amounts (50 µg) were loaded and confirmed with Tubulin and Tom20 for the cytosolic and mitochondrial fractions, respectively. \*p<0.05, when compared to CT cybrid group (Published by Santos et al, 2014).

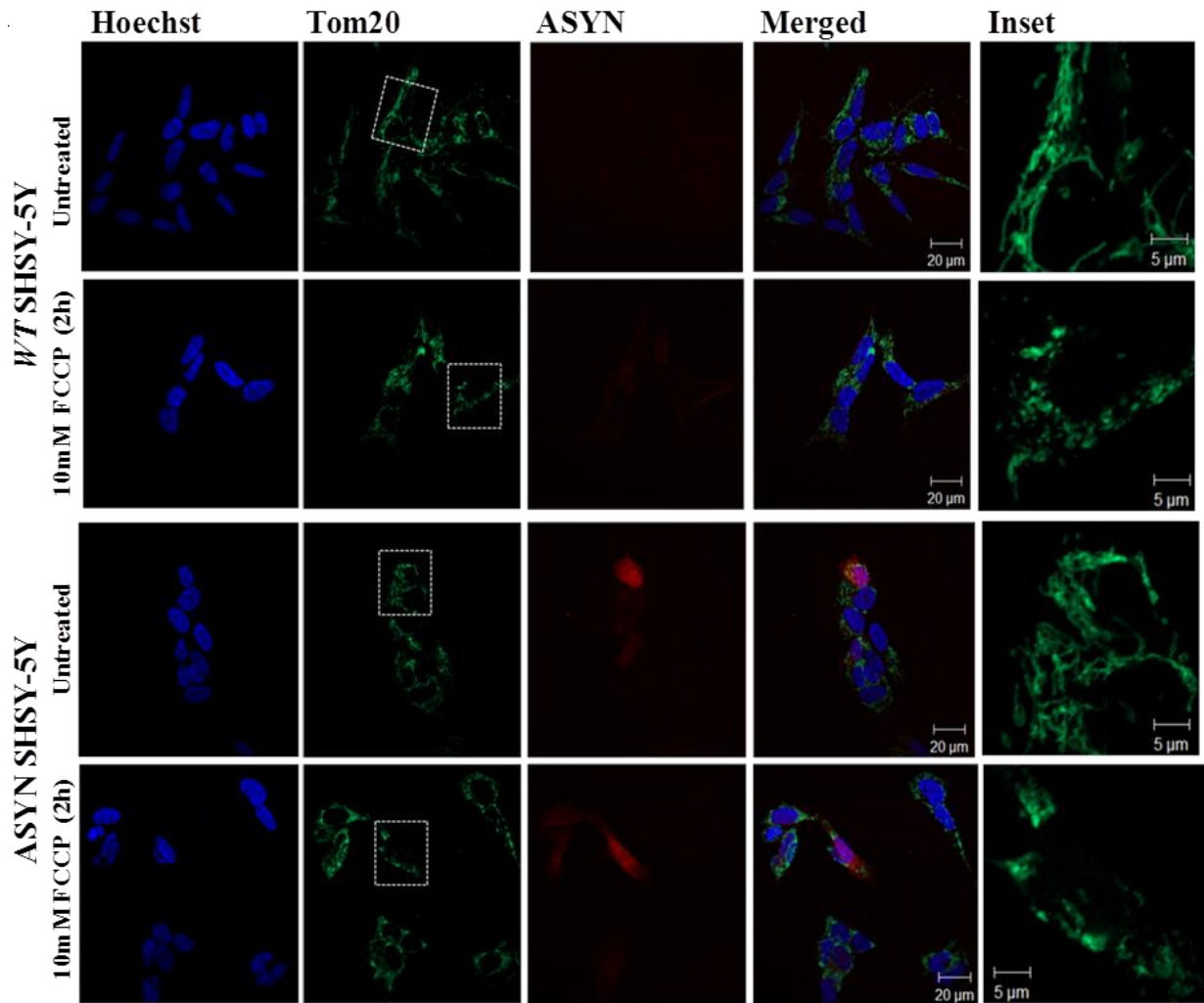


**Figure 6 - Mitochondrial fragmentation in ASYN overexpressing cells.**

Representative immunofluorescence pictures evidencing mitochondrial network in WT and ASYN overexpressing SHSY-5Y cells, under basal conditions, or treated with FCCP (10 $\mu$ M, 2 hours). Immunocytochemistry was performed against the mitochondrial protein Tom20 and  $\alpha$ -synuclein. ASYN overexpressing cells show an interconnected and elongated mitochondrial network, similar to what is observed in the WT cells, nevertheless, FCCP treated cells show mitochondrial fragmentation and perinuclear. (n=1). Green: Tom20, Red:  $\alpha$ -synuclein, Blue: Hoechst.

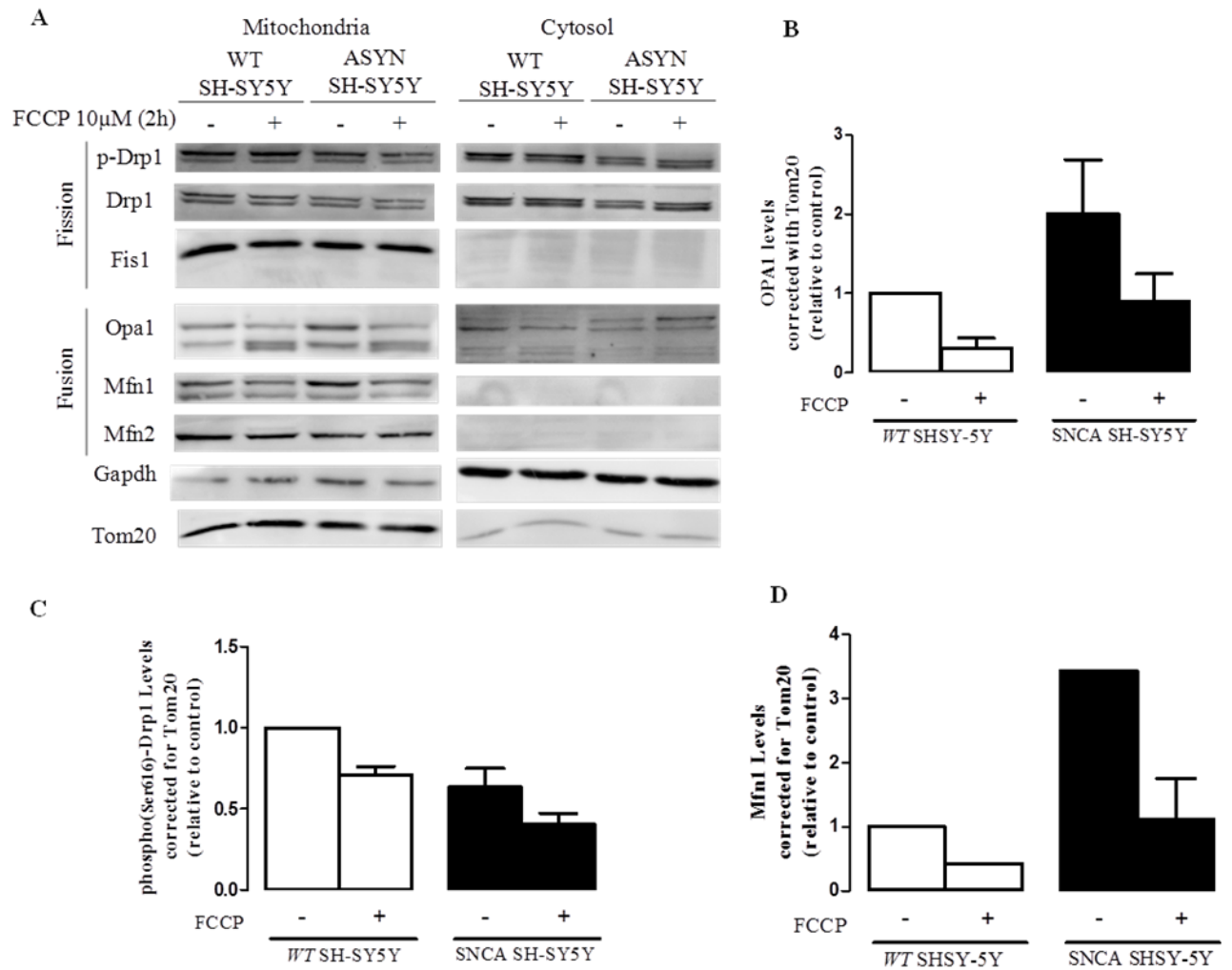


**Fig. 7 - Fusion and Fission protein expression levels in ASYN overexpressing cells.**

Cells were harvested and fractionated into mitochondrial and cytosolic fractions; A) Representative immunoblot; B-D) Densitometric analysis of the proteins levels involved in mitochondrial fission and fusion revealed an increase in the mitochondrial levels of the pro-fusion Opa1 (n=2) and Mfn1 (n=1-2) and a decrease of the pro-fission pDrp1 (n=2) levels in ASYN overexpressing cells. Equal protein amounts (50  $\mu$ g) were loaded and confirmed with  $\alpha$ -Tubulin and Tom20 for the cytosolic and mitochondrial fractions, respectively. The purity of the mitochondrial and cytosolic fractions is confirmed by the negligible contamination each fraction with the marker of the other fraction. Data represent mean  $\pm$  SEM values derived from two independent determinations

## DISCUSSION

The data presented in this work supports the idea that the inhibition of Lys40 of  $\alpha$ -tubulin and ASYN deacetylation provided by SIRT2 inhibition can be a possible weapon in the field of synucleinopathies, like PD. In fact we have shown that with this approach is possible to improve MT network, providing an improvement in autophagic flux and degradation of autophagic cargo, usually defective in PD. Autophagy has a huge importance in cellular homeostasis assuming valuable neuroprotective functions, simultaneously it is well established that autophagy is an energy sensitive process, in fact alterations in mitochondrial energy metabolism play an important role on the modulation of autophagy (39,40). Previous work from our group reported that pathways influenced by aerobic metabolism are altered in sPD cybrids, including autophagy (41,42). Moreover, our former studies revealed that autophagy failure stemming from mitochondrial dysfunction is not translated into defects in autophagosomes formation but mainly in the autophagosomes trafficking along the MT network towards the lysosomal compartment (35). Additionally, we also observed that in PD cells mitochondrial dysfunction can lead to a deficient ATP supply to microtubule protein motors leading to mitochondrial axonal transport disruption (43).

Taking these studies into account our major goal was to evaluate whether the stabilization of the impaired MT network could improve the autophagic process and work as a therapeutic strategy for neurodegenerative disorders such as PD. In this study we evidenced the role of SIRT2 in MT instability via  $\alpha$ -tubulin deacetylation. In fact,  $\alpha$ -tubulin acetylation is a post-translational modification that is a marker of stable microtubules (44). Furthermore we demonstrated the interplay between SIRT2, Tau and ASYN in cells harboring PD patient's mitochondria with mitochondrial deficits (PD cybrids) and ASYN overexpressing cells. We confirmed that Tau and ASYN are MT-associated proteins. In fact both Tau and ASYN have

been previously shown to be MT-associated/binding proteins (45). Moreover, SIRT2 is an active tubulin deacetylase whose inactivation leads to a great accumulation of acetylated MTs in our cellular models of PD. The biological relevance of  $\alpha$ -tubulin acetylation remains uncertain; however with this research we provide evidence that  $\alpha$ -tubulin acetylation is functionally associated with the improvement of intracellular trafficking, providing a better autophagic turnover. In fact, elevation of MT acetylation by the selective inhibition of SIRT2 catalytic activity enhanced MT-directed transport of autophagic vacuoles towards the lysosomal compartment as it was evidenced by the great increase in the autophagic flux in PD cybrids and ASYN overexpressing cells. These data are consistent with previous reports demonstrating that ASYN-mediated neurotoxicity in several models of PD is partially due to deacetylation of  $\alpha$ -tubulin by SIRT2 (14). The selective inhibition of SIRT2 ascertained by this work also provided other arguments that corroborate this approach as a possible new therapeutic strategy for PD, in fact we observed decreased levels of pTau which is associated with the improvement of MT dynamic, moreover we showed that the treatment with AK1 enhanced the interaction between these Tau and ASYN and MTs which increases the stability of MT network. Additionally, the treatment with AK1 also increased the ASYN acetylation levels, which can work as a protective factor against ASYN aggregation (46).

Mitochondrial dysfunction is characterized by an imbalance between mitochondrial fission and fusion process and oxidative stress. Together with other deficits, mitochondrial dysfunction has been extensively associated with several neurodegenerative diseases, including sPD (5). In order to elucidate that, we wanted to assess whether MT-dependent mitochondrial dynamics is altered in PD cells with inherent mitochondrial dysfunction as well as in ASYN overexpressing cells, since both mitochondrial deficits and ASYN accumulation are cellular hallmarks of PD. With this study we have demonstrated the role of the proteins involved in mitochondrial fusion/fission process in mitochondrial interconnectivity, showing

that abnormal mitochondrial distribution and morphology is a consequence of OXPHOS deficiency in sPD cybrids. Indeed, we have shown that PD cybrids with OXPHOS deficiency have abnormal mitochondria localization and an increase fragmentation pattern, resulting in the appearance of round-shaped disconnected mitochondria. We additionally have found that in PD cells the increase in mitochondrial fission was due to an increase in mitochondrial Drp 1 phosphorylated levels and Opa1 long isoform (LI) cleavage. In contrast, ASYN overexpressing cells have a more elongated mitochondrial network due to an increase in mitochondrial Opa1 levels and to a decrease in pDrp1 levels. These data indicate that a differential regulation of fusion-fission events seems to occur in sPD and ASYN overexpressing cells.

## **CONCLUSION**

In summary, data reported in this work strongly support that a compromised mitochondrial dynamics and disassembled MT network, probably supplied by the deacetylation provided by SIRT2, appear to compromise quality control autophagy. Ultimately, these deficits potentiate the accumulation of ASYN oligomers, as well as, impaired mitochondria and autophagic vesicles finally prompting apoptosis. This study indicates that therapeutic modulation, aiming MT and ASYN acetylation could be a great advance in the field of neurodegenerative disorders, like sPD.

## REFERENCES

1. L.S.Forno. Neurophatology of Parkinson's disease. , Journal of Neuropathology and Experimental Neurology, vol.55, no. 3, pp. 259-272; 1996.
2. A. H. V. Schapira, J. M. Cooper, D. Dexter, P. Jenner, J. B. Clark, and C. D. Marsden. "Mitochondrial complex I deficiency in Parkinson's disease". Lancet, vol. 1, no. 8649; 1989.
3. W. D. Parker, S. J. Boyson, and J. K. Parks. Abnormalities of the electron transport chain in idiopathic Parkinson's disease. Annals of Neurology, vol. 26, no. 6, pp. 719–723, 1989.
4. Swerdlow, R.H., Parks, J.K., Miller, S.W., Tuttle, J.B., Trimmer, P.A., Sheehan, J.P., Bennett, J.P., Jr., Davis, R.E. and Parker, W.D., Jr. Origin and functional consequences of the complex I defect in Parkinson's disease. , Ann. Neurol., 40, 663-671; 1996.
5. Cardoso, S.M. The mitochondrial cascade hypothesis for Parkinson's disease. Curr. Pharm. Des., 17, 3390-3397; 2011.
6. Swerdlow, R.H. Does mitochondrial DNA play a role in Parkinson's disease? A review of cybrid and other supportive evidence.. Antioxid. Redox Signal., 16, 950-964; 2012.
7. Santos D, Cardoso SM. Mitochondrial dynamics and neuronal fate in Parkinson's disease. Mitochondrion 12:428–437; 2012.
8. Westermann B. Mitochondrial fusion and fission in cell life and death. Nat Rev Mol Cell Biol11:872–884; 2010.
9. Arduino DM, Esteves AR, Cardoso SM. Mitochondrial fusion/fission, transport and autophagy in Parkinson's disease: when mitochondria get nasty. Parkinsons Dis 2011:767230; 2011.
10. Su B, Wang X, Zheng L, Perry G, Smith MA, Zhu X. Abnormal mitochondrial dynamics and neurodegenerative diseases. Biochim Biophys Acta 1802:135–142; 2010.
11. Chen H, Chan DC. Mitochondrial dynamics—fusion, fission, movement, and mitophagy—in neurodegenerative diseases. , HumMol Genet 18:R169–R176; 2009.
12. Ishihara N, Fujita Y, Oka T, Mihara K. Regulation of mitochondrial morphology through proteolytic cleavage of OPA1. , EMBO J 25:2966–2977; 2006.
13. G. Schiavo, M. Fainzilber. Cell biology: alternative energy for neuronal motors. , Nature 495 (2013) 178–180.

14. Outeiro, T.F., Kontopoulos, E., Altmann, S.M., Kufareva, I., Strathearn, K.E., Amore, A.M., Volk, C.B., Maxwell, M.M., Rochet, J.C., McLean, P.J., et al. Sirtuin 2 inhibitors rescue alpha-synuclein-mediated toxicity in models of Parkinson's disease. *Science* 317, 516-519; 2007.
15. North, B.J., Marshall, B.L., Borra, M.T., Denu, J.M., and Verdin, E. The human Sir2 ortholog, SIRT2, is an NAD<sup>+</sup>-dependent tubulin deacetylase. *Molecular cell* 11, 437-444; 2003.
16. North, B.J., and Verdin, E. Mitotic regulation of SIRT2 by cyclin-dependent kinase 1-dependent phosphorylation. *The Journal of biological chemistry* 282, 19546-19555; 2007.
17. Hubbert, C., Guardiola, A., Shao, R., Kawaguchi, Y., Ito, A., Nixon, A., Yoshida, M., Wang, X.F., and Yao, T.P. HDAC6 is a microtubule-associated deacetylase. *Nature* 417, 455-458.; 2002.
18. Matsuyama, A., Shimazu, T., Sumida, Y., Saito, A., Yoshimatsu, Y., Seigneurin-Berny, D., Osada, H., Komatsu, Y., Nishino, N., Khochbin, S., et al. In vivo destabilization of dynamic microtubules by HDAC6-mediated deacetylation. , *The EMBO journal* 21, 6820-6831; 2002.
19. Haggarty, S.J., Koeller, K.M., Wong, J.C., Grozinger, C.M., and Schreiber, S.L. Domain-selective small-molecule inhibitor of histone deacetylase 6 (HDAC6)-mediated tubulin deacetylation. , *Proceedings of the National Academy of Sciences of the United States of America* 100, 4389-4394; 2003.
20. Narhi et al. Both Familial Parkinson's Disease Mutations Accelerate  $\alpha$ -Synuclein Aggregation. *The Journal of Biological Chemistry*, 274, 9843-9846; 1999.
21. I. Litvan. Update on epidemiological aspects of progressive supranuclear palsy. , *Mov. Disord.* 18 (Suppl. 6) (2003) S43–S50.
22. D. Krige, M.T. Carroll, J.M. Cooper, C.D. Marsden, A.H. Schapira. Platelet mitochondrial function in Parkinson's disease. *The Royal Kings and Queens Parkinson Disease Research Group, Ann. Neurol.* 32 (1992) 782–788.
23. M.M. Bradford. A rapid and sensitive method for the quantitation of microgram quantities of protein utilizing the principle of protein-dye binding. *Anal. Biochem.* 72 (1976) 248–254.
24. C. Sodja, H. Fang, T. Dasgupta, M. Ribocco, P.R.Walker, M. Sikorska, *Brain Res.* Identification of functional dopamine receptors in human teratocarcinoma NT2 cells. , *Mol. Brain Res.* 99 (2002) 83–91.
25. I.E. Misiuta, S. Saporta, P.R. Sanberg, T. Zigova, A.E. Willing. Influence of retinoic acid

- and lithium on proliferation and dopaminergic potential of human NT2 cells. *J. Neurosci. Res.* 83 (2006) 668–679.
- R.H. Swerdlow, J.K. Parks, D.S. Cassarino, D.J. Maguire, R.S. Maguire, J.P. Bennett Jr.,  
 26. R.E. Davis, W.D. Parker Jr. Cybrids in Alzheimer's disease: a cellular model of the disease. , *Neurology* 49 (1997) 918–925.
- D.R. Binder, W.H. Dunn Jr., R.H. Swerdlow. Molecular characterization of mtDNA  
 27. depleted and repleted NT2 cell lines. *Mitochondrion* 5 (2005) 255–265.
- S.M. Cardoso, A.C. Rego, N. Penacho, C.R. Oliveira. Apoptotic cell death induced by  
 28. hydrogen peroxide in NT2 parental and mitochondrial DNA depleted cells. *Neurochem. Int.* 45 (2004) 693–698.
- S.W. Miller, P.A. Trimmer, W.D. Parker Jr., R.E. Davis. Creation and characterization of  
 29. mitochondrial DNA-depleted cell lines with “neuronal-like” properties. *J. Neurochem.* 67 (1996) 1897–1907.
- R.H. Swerdlow, J.K. Parks, S.W. Miller, J.B. Tuttle, P.A. Trimmer, J.P. Sheehan, J.P.  
 30. Bennett Jr., R.E. Davis, W.D. Parker Jr.. Origin and functional consequences of the complex I defect in Parkinson's disease. *Ann. Neurol.* 40 (1996) 663–671.
- D.M. Arduino, A.R. Esteves, L. Cortes, D.F. Silva, B. Patel, M. Grazina, R.H. Swerdlow,  
 31. C.R. Oliveira, S.M. Cardoso. Mitochondrial metabolism in Parkinson's disease impairs quality control autophagy by hampering microtubule-dependent traffic. *Hum. Mol. Genet.* 21 (2012) 4680–4702.
- R.K. Dagda, S.J. Cherra III, S.M. Kulich, A. Tandon, D. Park, C.T. Chu. Loss of PINK1  
 32. function promotes mitophagy through effects on oxidative stress and mitochondrial fission. *J. Biol. Chem.* 284 (2009) 13843–13855.
- Drewes G., Trinczek B., Illenberger S., Biernat J., Schmitt-Ulms G., Meyer H. E.,  
 Mandelkow E.-M., and Mandelkow E. Microtubule-associated protein/microtubule  
 33. affinity-regulating kinase (p110mark). A novel protein kinase that regulates tau–microtubule interactions and dynamic instability by phosphorylation at the Alzheimer-specific site serine 262. , *J. Biol. Chem.* 270, 7679–7688; 1995.
- Fass, E., Shvets, E., Degani, I., Hirschberg, K., and Elazar. Microtubules support  
 34. production of starvation-induced autophagosomes but not their targeting and fusion with lysosomes. *The Journal of biological chemistry* 281, 36303–36316; 2006.
- Arduino, D.M., Esteves, A.R., Cortes, L., Silva, D.F., Patel, B., Grazina, M., Swerdlow,  
 35. R.H., Oliveira, C.R., and Cardoso, S.M. Mitochondrial metabolism in Parkinson's disease impairs quality control autophagy by hampering microtubule-depend. ; 2012.

- J. W. Langston, P. Ballard, J. W. Tetrud, and I. Irwin. Chronic parkinsonism in humans  
36. due to a product of meperidine-analog synthesis. , *Science*, vol. 219, no. 4587, pp. 979–980, 1983.
37. Przedborski, S., Tieu, K., Perier, C., Vila, M. MPTP as a mitochondrial neurotoxin model of Parkinson's disease. , *J. Bioener. Biomembr.* 36, 375–379.; 2004.
38. Mochizuki, H., Goto, K., Mori, H., Mizuno, Y. Histochemical detection of apoptosis in Parkinson's disease. , *J. Neurol. Sci.* 137, 120–123; 1996.
39. Arduíno DM et al. Mitochondria drive autophagy pathology via microtubule disassembly: a new hypothesis for Parkinson disease. *Autophagy*; 2013.
40. Klionsky DJ et al. Guidelines for the use and interpretation of assays for monitoring autophagy. , *Autophagy*; 2012.
41. A. Raquel F. Esteves, A. Filipa Dominguesa, I. Luísa Ferreira, Cristina Januário, Russell H. Swerdlow, Catarina R. Oliveira, Sandra M. Cardoso. Mitochondrial function in Parkinson's disease cybrids containing an nt2 neuron-like nuclear background. *Mitochondrion.* 8:219-228; 2008.
42. A. Raquel Esteves, Jane Lu, Mariana Rodova, Isaac Onyango, E Lezi, Richard Dubinsky, Kelly E. Lyons, Rajesh Pahwa, Jeffrey M. Burns, Sandra M. Cardoso and Russell H. Swerdlow. Mitochondrial respiration and respiration-associated proteins in cell lines created through Parkinson's subject mitochondrial transfer. *J.Neurochem.* 113:674-682; 2010.
43. Esteves AR, Arduíno DM, Swerdlow RH, Oliveira CR, Cardoso SM. Microtubule Depolymerization Potentiates Alpha-Synuclein Oligomerization. , *Frontiers in Aging Neuroscience* 2009;1:5.
44. Janke C, Bulinski JC. Post-translational regulation of the microtubule cytoskeleton: mechanisms and functions. , *Nat Rev Mol Cell Biol* 2011, 12: 773-786.
45. Alim, M.A., Ma, Q.L., Takeda, K., Aizawa, T., Matsubara, M., Nakamura, M., Asada, A., Saito, T., Kaji, H., Yoshii, M., et al. Demonstration of a role for alpha-synuclein as a functional microtubule-associated protein. *Journal of Alzheimer's disease : JAD* 6, 435-442; discussion 443-439; 2004.
46. Bartels T, Kim NC, Luth ES, Selkoe DJ. N-Alpha-Acetylation of  $\alpha$ Synuclein Increases Its Helical Folding Propensity, GM1 Binding Specificity and Resistance to Aggregation. , *PLoS ONE* 9(7): e103727; 2014.